B-Staged Epoxy/Single-Walled Carbon Nanotube Nanocomposite Thin Films for Composite Reinforcement

Graham L. Warren,[1] Luyi Sun,[1] Viktor G. Hadjiev,[2] Daniel Davis,[3] Dimitris Lagoudas,[3] Hung-Jue Sue[1]

[1]*Polymer Technology Center, Department of Mechanical Engineering, Texas A&M University, College Station, Texas 77843-3123*
[2]*Texas Center for Superconductivity and Department of Mechanical Engineering, University of Houston, Houston, Texas 77204-5002*
[3]*Department of Aerospace Engineering, Texas A&M University, College Station, Texas 77843-3141*

Received 12 March 2008; accepted 23 May 2008
DOI 10.1002/app.29375
Published online 29 December 2008 in Wiley InterScience (www.interscience.wiley.com).

ABSTRACT: B-staged epoxy/single-walled carbon nanotube (SWCNT) nanocomposite thin films at 50% cure were prepared to improve the conductivity and mechanical performance of laminated composites. The SWCNTs were functionalized by oxidation and subsequent grafting with polyamidoamine generation-zero dendrimers. The epoxy nanocomposites containing SWCNTs were successfully cast into thin films by the manipulation of the degree of cure and the viscosity of the epoxy. Raman microscopy characterization revealed that the thin films exhibited a high degree of SWCNT dispersion in the epoxy. The B-staged thin films were seamlessly integrated into laminated composite systems upon heating and could serve as interleaves to improve the conductivity and mechanical strength of laminated fiber composite systems. © 2008 Wiley Periodicals, Inc. J Appl Polym Sci 112: 290–298, 2009

Key words: dispersions; films; mechanical properties; Raman spectroscopy; resins

INTRODUCTION

Since their discovery,[1] carbon nanotubes, especially single-walled carbon nanotubes (SWCNTs), have attracted significant interest because of their remarkable properties.[2–5] Among a wide range of applications, SWCNTs have been considered as ideal reinforcing agents for composite applications[6] because of their superior Young's modulus ($\sim$ 1 TPa)[7] and high aspect ratio[8] values. In addition to their extremely high modulus and strength values, SWCNTs possess a high electrical conductivity ($>10^4$ S/cm)[9] and thermal conductivity (>2000 W $m^{-1}{\cdot}K^{-1}$),[10] which enable the preparation of multifunctional high-performance polymer composites. In recent years, SWCNT-based polymer nanocomposites have been extensively studied through the use of a wide range of polymer matrices,[11–13] which have included epoxy,[14–16] polypropylene,[17] polyethylene,[18] poly(methyl methacrylate),[19] polyacrylonitrile,[20] and poly(vinyl alcohol),[21] for various structural and functional applications.

To fully impart the unique properties of SWCNTs into polymers, it is critical to achieve (1) good dispersion of the SWCNTs in the polymer matrices, (2) strong adhesion between the SWCNTs and the matrix, and (3) alignment of the SWCNTs.[11,12] Vast research efforts have been made to address these needs, among which the surface functionalization of SWCNTs is an attractive approach because it can address both the dispersion and adhesion attributes. Both covalent and noncovalent functionalization methods have been extensively studied and developed over the years.[13] Each method has its own advantages and disadvantages.

In most polymer/SWCNT nanocomposites, it is desirable to prepare uniformly dispersed SWCNTs in a polymeric matrix to achieve an overall high material performance and multifunctionality. However, a high concentration of SWCNTs in the matrix would usually be needed to do so. This, in turn, would lead to a significant increase in cost and a compromise in processability, especially for the fabrication of laminated composites by vacuum-assisted resin transfer molding (VARTM). Alternative approaches have to be undertaken to strategically place SWCNTs in locations of interest within the composite system.

Correspondence to: H.-J. Sue (hjsue@tamu.edu).
Contract grant sponsor: U.S. Air Force AFRL; contract grant number: FA8650-05-D-1912 (Minority Leaders Program).
Contract grant sponsor: State of Texas through the Texas Center for Superconductivity, University of Houston (partial support to V.G.H.).

In this article, a new strategy for the placement of epoxy nanocomposites with a high content of SWCNT at the location of interest via the preparation of partially cured (B-staged) epoxy/SWCNT thin films is reported. Because the films are partially cured, the SWCNTs are locked in place, even after they are subsequently cocured and integrated with neat epoxy. Because the thin films are prepared separately, higher SWCNT loadings can be incorporated into the polymer matrix without a sacrifice of processability, especially for the VARTM process. Thus, desirable properties, such as good mechanical strength and high electrical/thermal conductivities, can be achieved at the location of interest at a much lower cost.

Specifically, B-staged thin films are to be used as interleaves to enhance the conductivity, interlaminar strength, and toughness of laminated VARTM composites.[22–27] The increase in the interlaminar strength and toughness can, in turn, improve the compression after impact strength of the composites.[22,26] Thus, thin films containing well-dispersed SWCNTs, which usually exhibit improved modulus and toughness,[11] appear to be ideal candidates for the reinforcement of laminated composites. As described in the literature, a number of approaches have been developed to incorporate nanotubes into laminated composites and have been shown to be effective.[28] However, these approaches require the incorporation of nanotubes into the entire composite system[28] or the spraying of SWCNTs onto the substrate;[29,30] these methods are not practical for large-scale VARTM productions. The approach proposed in this article to introduce a high concentration of SWCNTs into desired composite laminate locations is expected not only to help address the interlaminar strength improvement needs but also to bring about SWCNT functionalities, such as high electrical and thermal conductivity, for aerospace composite applications.

In addition to the interleaf composite applications mentioned previously, epoxy/SWCNT nanocomposite thin films may find a variety of other applications, such as microdevices and electronic packaging[31–33] and coatings for corrosion protection.[34] If SWCNT alignment can be achieved during processing, significantly more applications can be expected.[11]

In this study, a covalent functionalization approach was adopted to treat the SWCNTs for the preparation of the epoxy/SWCNT nanocomposite thin films. Detailed steps for the preparation of the B-staged thin films with uniform thicknesses are described. The quality of the dispersion of the SWCNTs in the epoxy and the degree of cure were determined with Raman spectroscopy and differential scanning calorimetry (DSC), respectively. The usefulness of B-stage thin films for laminated composite applications is discussed.

EXPERIMENTAL

Materials

The epoxy resin and curing agent used in this study were EPIKOTE 862 resin (formerly Epon 862) and EPIKURE W curing agent (formerly Epicure W), both of which were obtained from Hexion Specialty Chemicals, Inc. (Columbus, OH). The SWCNTs (XD grade) were provided by Carbon Nanotechnologies, Inc. (Houston, TX), and had a reported density of about 1.35 g/cm^3 and an aspect ratio of greater than 1000. The polyamidoamine (PAMAM) generation-zero (G0) dendrimer was purchased from Sigma-Aldrich. Concentrated sulfuric acid (95.4%) and nitric acid (70%) were obtained from Fisher Scientific. Poly(vinylidene difluoride) filter membranes with a pore size of 45 μm were purchased from Millipore (Billerica, MA). The thin-film coater, to which a temperature control system was later added in our laboratory, was purchased from Elcometer, Inc. (Rochester Hills, MI). The release paper was donated by Hexcel Corp. (Salt Lake City, UT). All of the chemicals were used as received.

Functionalization of the SWCNTs

A sample of 1.0 g of SWCNTs was first oxidized by a mixture of 180 mL of concentrated sulfuric acid and 60 mL of concentrated nitric acid in a round-bottom flask. The mixture was ultrasonicated in an ultrasonication bath for 2.5 h. After sonication, 760 mL of deionized water was added to the sample, and the system was sonicated for an additional 3 h. Oxidized single-walled carbon nanotubes (O-SWCNTs) were obtained in this step. The O-SWCNT sample was then collected through a poly(vinylidene difluoride) filter membrane and washed several times with deionized water to remove acid residues. The cleaned O-SWCNTs were then redispersed in acetone by an additional 3 h of sonication. The O-SWCNTs were further treated by interaction with the PAMAM G0 dendrimer. The corresponding amount of PAMAM G0 dendrimer, which was determined by the degree of oxidation on the SWCNT surface,[35] was added to the O-SWCNT sample dispersed in acetone; this was followed by 1 h of sonication to ensure good mixing and interaction. Details of the interaction between O-SWCNT and the PAMAM G0 dendrimer to form PAMAM G0 functionalized single-walled carbon nanotubes (F-SWCNTs) can be found elsewhere.[35]

Preparation of the epoxy/SWCNT nanocomposite thin films

The F-SWCNTs, which were well dispersed in acetone, were then added to the epoxy monomer at a

predetermined ratio and sonicated for 15 min to achieve a final SWCNT loading of 0.5 wt % in the final nanocomposite. Multiple samples were prepared in conjunction with the multiple states of SWCNT treatment. The three states of SWCNT used were the pristine single-walled carbon nanotube (P-SWCNT), O-SWCNT, and F-SWCNT. The three epoxy/nanocomposite samples prepared were epoxy/P-SWCNT, epoxy/O-SWCNT, and epoxy/F-SWCNT, respectively. After the removal of acetone with a rotary evaporator in a water bath at 70°C, the curing agent was added (26.4 parts by weight/100 parts by weight of EPIKOTE 862). The epoxy/SWCNT mixture was further degassed to remove the remaining air bubbles trapped within the sample.

The samples were then B-stage cured at 121°C for 70 min in an oven. Before removal of the epoxy/SWCNT samples from the oven, the thin-film coater was preheated to 90°C. The epoxy/SWCNT samples were quickly transferred from the oven and immediately cast into thin films at a thickness of 50 μm on release paper, which was laid on the thin film coater. For comparison purposes, B-stage-cured neat epoxy thin films were also prepared with the same procedures.

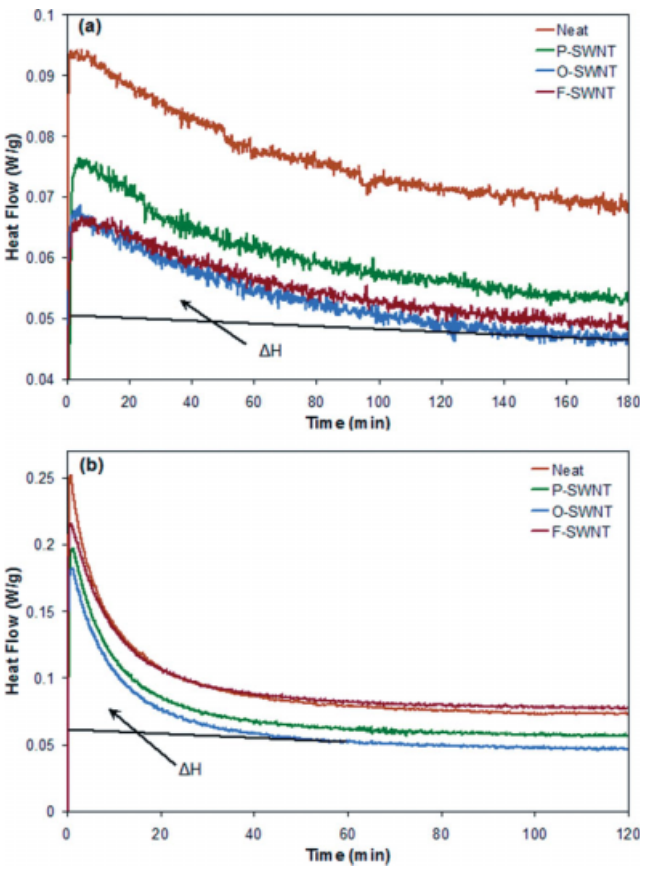

Figure 1 DSC thermograms of the epoxy/SWCNT nanocomposite thin films: samples cured at (a) 121°C for 3 h and (b) 177°C for 2 h (ΔH = exotherm during curing). [Color figure can be viewed in the online issue, which is available at www.interscience.wiley.com.]

TABLE I
Time Required to Achieve a 50% B-Stage Cured Thin Film at a Thickness of 50 μm

Sample (0.5 wt %)	Curing temperature (°C)	Duration of curing (min)	Degree of curing (%)
Neat epoxy	121	70	50.1
Epoxy/P-SWCNT	121	60	31.1
Epoxy/O-SWCNT	121	75	67.4
Epoxy/F-SWCNT	121	65	41.1
Epoxy/F-SWCNT	121	70	50.9

Characterization

A Mettler Toledo (Columbus, OH) (model DSC821^e) differential scanning calorimeter was used to obtain DSC thermograms. The samples were kept isothermal at 121°C for 70 min to mimic the B-stage curing process in the oven and kept isothermal at 177°C for 2 h to mimic the complete curing condition. The experiments were carried out under a nitrogen gas purge (80 mL/min).

Raman and optical microscopy were used to assess and visualize the dispersion and distribution of SWCNTs in the epoxy matrix. The Raman microscope consisted of a T64000 Horiba JY (Edison, NJ) triple spectrometer coupled to a confocal optical microscope furnished with an XYZ motorized stage. A microscope objective (50×) was used to focus the 632.8-nm laser beam to a focal cylinder about 1.5 μm in diameter and about 7 μm in height, with the latter given by the depth of focus. The confocal layout of the microscope ensured that only light scattered within the confocal cylinder was directed to the spectrometer. The focused laser beam was raster-scanned on the sample surface, and a Raman spectrum excited at each step of the scan was recorded for parallel-incident and scattered-light polarizations. The collected data formed a hyperspectral cube of the scanned area, which contained both spectral and spatial information.

Tensile property testing of the epoxy/SWCNT nanocomposites was carried out on the basis of the ASTM D 638-98 method. The epoxy/SWCNT was prepared in panels 3 mm thick to test their bulk properties. The tensile tests were performed with an MTS (Eden Prairie, MN) servohydraulic testing machine at a crosshead speed of 5.08 mm/min at ambient temperature. The Young's modulus, tensile strength, and elongation at break of each sample were obtained on the basis of at least five specimens per sample. The average values and standard deviations are reported.

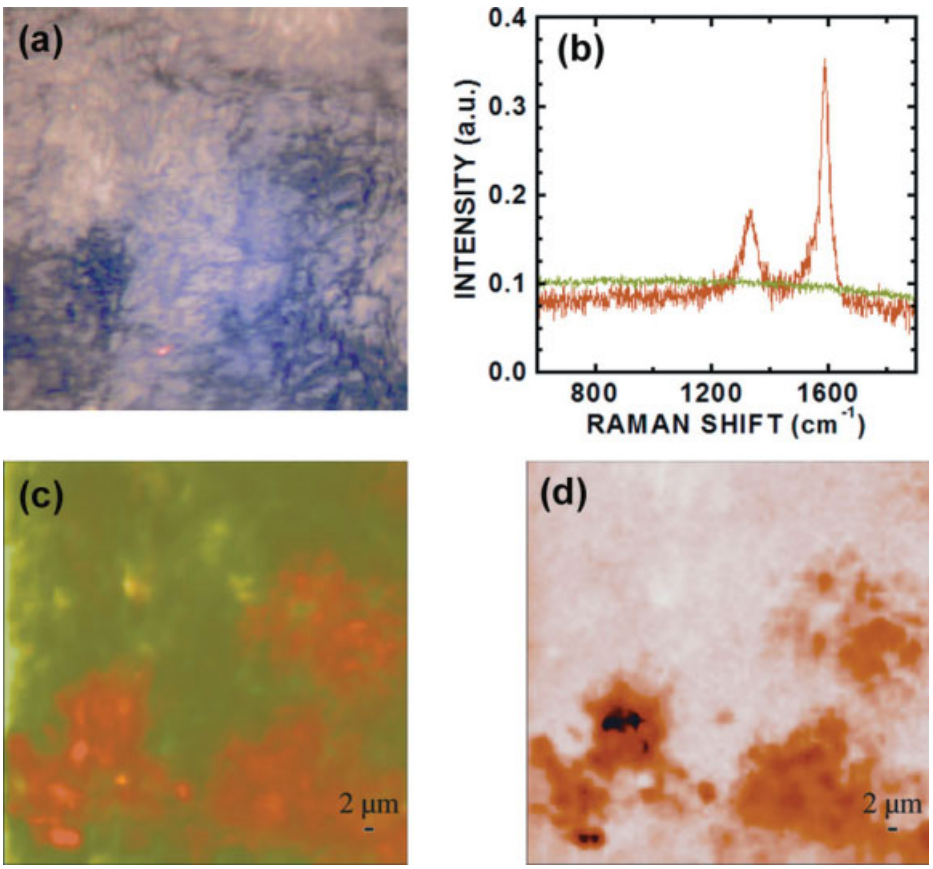

Figure 2 (a) Optical image of an 80 × 80 μm^2 area on the surface of an epoxy/P-SWCNT (0.5 wt %) nanocomposite thin film. (b) Reference Raman spectra of the P-SWCNT (orange color) and epoxy matrix (green color) used to produce (c) the Raman image; brighter colors denote a higher intensity. (d) G-band intensity distribution; the darker color corresponds to a higher intensity. [Color figure can be viewed in the online issue, which is available at www.interscience.wiley.com.]

RESULTS AND DISCUSSION

Film preparation

The film preparation was successful in the achievement of visually defect-free B-staged thin films. This effective approach involved the B-stage curing of the epoxy samples in an oven, followed by the formation of the B-stage thin films with a commercial film coater. Numerous difficulties had to be overcome to prepare good quality epoxy/SWCNT thin films. With the addition of SWCNTs to the epoxy, there was a significant increase in viscosity of the sample. How well B-stage thin films are prepared depends strongly on the control of the nanocomposite viscosity. If the viscosity of the B-staged sample is too high, significant film defects on the surface form. If the viscosity is too low, voids appear in the thin film after film formation. In this research, after B-staged curing, the sample still possessed sufficient fluidity for thin-film casting while being able to maintain a relatively high viscosity to prevent void formation. Maintaining the thin film coater at an appropriate temperature (90°C in this case) was also critical for the film casting to prevent the epoxy/SWCNT nanocomposite from excessive hardening, which thus preserved the formability of the films during the film-casting process.

Therefore, the key for successful thin-film preparation was the balance of the degree of cure and viscosity of the sample. Control of the degree of cure is important for the preparation of B-staged thin films. The two main factors that affect the degree of cure are the temperature and duration of the curing reaction. Too high a degree of cure results in a high viscosity, which negatively affects the thin-film formation process and also limits the cocuring and integration of the thin films with the injected epoxy monomers in the VARTM mold. In the case of viscosity control, all factors that can affect the system viscosity should be carefully controlled, including the dispersion and distribution of SWCNTs, concentration of SWCNTs, degree of cure, and casting temperature (coater temperature).

In this study, a 50% degree of cure for the epoxy samples appeared to be ideal for the handling, insertion, and integration of the thin films for VARTM

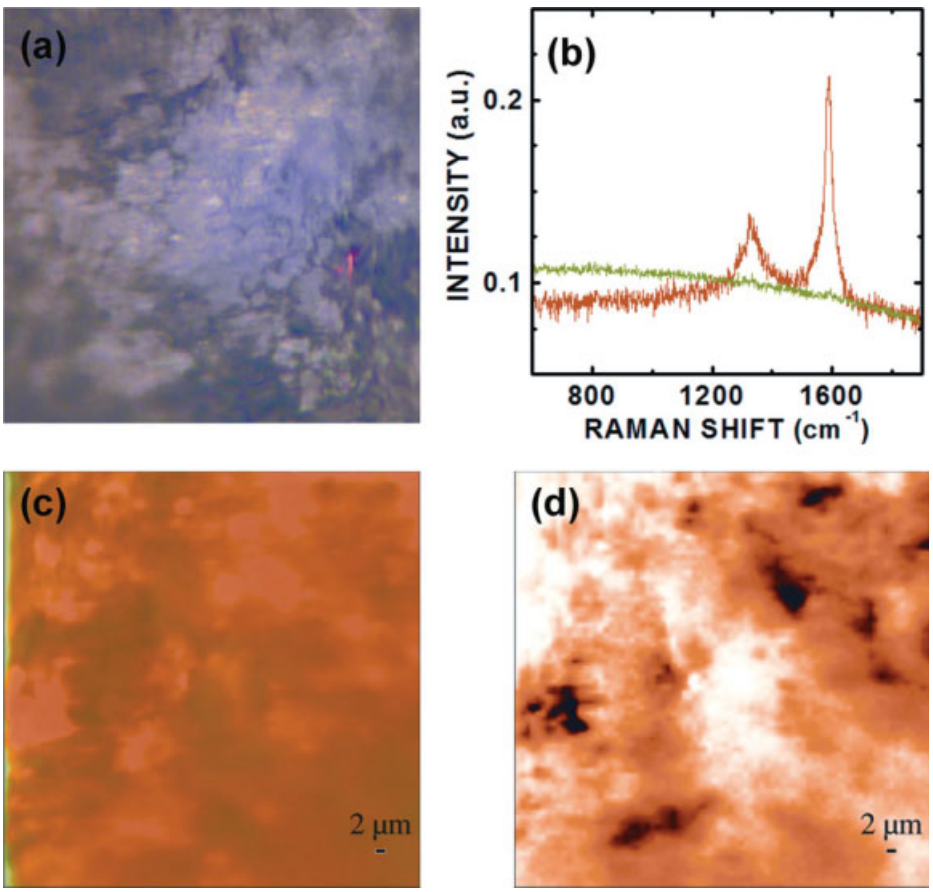

Figure 3 (a) Optical image of an 80 × 80 μm^2 area on the surface of an epoxy/O-SWCNT (0.5 wt %) nanocomposite thin film. (b) Reference Raman spectra of the O-SWCNT (orange color) and epoxy matrix (green color) used to produce (c) the Raman image; brighter colors denote a higher intensity. (d) G-band intensity distribution; the darker color corresponds to a higher intensity. [Color figure can be viewed in the online issue, which is available at www.interscience.wiley.com.]

composite reinforcement. However, for other material systems and applications, other sets of processing parameters may need to be used to prepare good quality thin films for intended applications.

Control and monitoring of the thin-film curing process

Generally speaking, the achievement of around 50% of epoxy curing in the final thin films is desired to allow for the B-stage-cured samples to cocure with the newly injected epoxy monomers and curing agent. In the meantime, at a 50% level of curing, the well-dispersed SWCNTs in the epoxy thin film remain locked in place in the interlaminar region to help increase the interlaminar strength and thermal/electrical conductivity.

The curing processes of the epoxy samples were monitored by DSC. The degree of cure was estimated by the ratio of the exotherm during the B-staged curing to the exotherm during the complete cure of the same sample, as shown in Figure 1. The DSC results show that the epoxy was almost 100% cured at 177°C for 90 min but requires a much longer curing time at 121°C. For the epoxy nanocomposite systems investigated here, it was determined that 70 min at 121°C yielded approximately a 50% cure of the samples (Table I). The incorporation of 0.5 wt % SWCNTs in epoxy was found to have little effect on the overall curing process.

The previous methodology gave rise to good quality B-staged thin films. The epoxy thin films containing P-SWCNT, O-SWCNT, and F-SWCNT exhibited similar visual appearances. All of the film samples could be easily handled and placed in the interlaminar regions of the laminated composites for VARTM processing.

Dispersion of the SWCNTs

The achievement of a high degree of dispersion of SWCNTs in epoxy is crucial for producing nanocomposites with desirable properties. Typical SWCNT aggregates are micrometers in size. Their dispersion

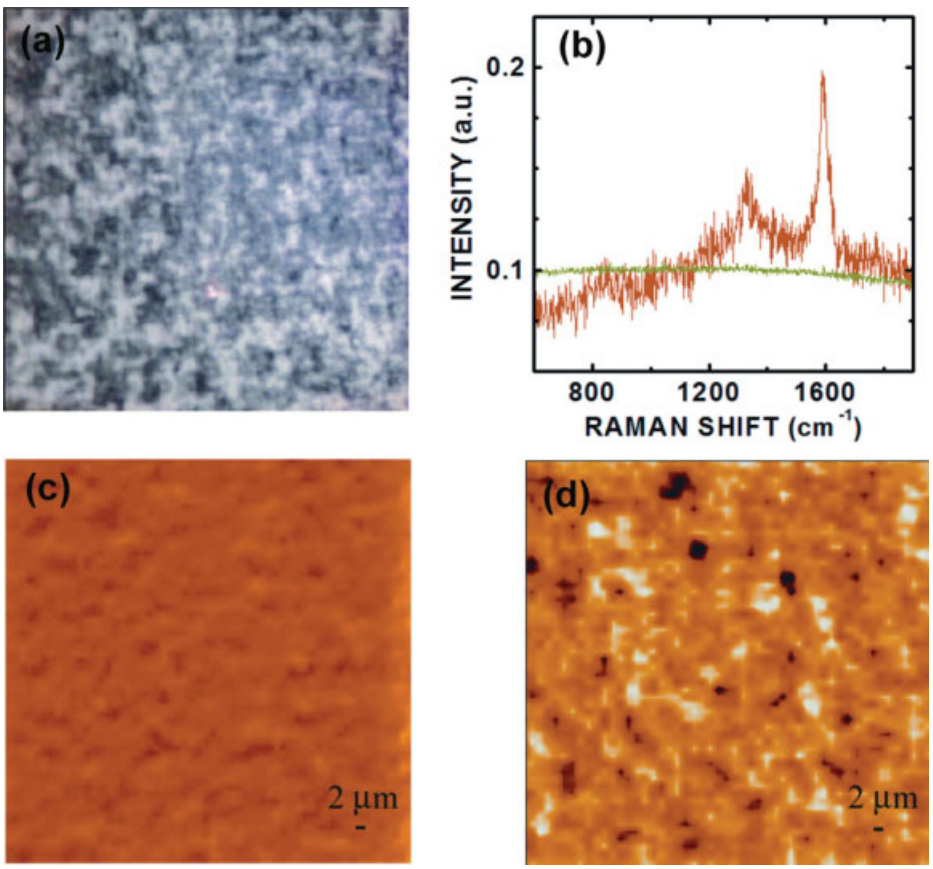

Figure 4 (a) Optical image of a 60 × 60 μm^2 area on the surface of an epoxy/F-SWCNT (0.5 wt %) nanocomposite thin film. (b) Reference Raman spectra of the F-SWCNT (orange color) and epoxy matrix (green color) used to produce (c) the Raman image; brighter colors denote a higher intensity. (d) G-band intensity distribution; the darker color corresponds to a higher intensity. [Color figure can be viewed in the online issue, which is available at www.interscience.wiley.com.]

is also generally poor. These imperfections can significantly compromise the nanocomposite properties, especially the mechanical properties. A high degree of dispersion of SWCNTs in thin-film interleaves is needed to achieve high compression after impact strength in composites.[26]

The oxidation of SWCNTs and the following reaction with the PAMAM G0 dendrimer has been shown to be an effective approach to functionalize SWCNTs, especially for the preparation of epoxy-based nanocomposites.[35] The dispersion and distribution of SWCNTs in the polymer matrix have been mainly characterized by scanning electron microscopy and transmission electron microscopy.[11–13,35] In this study, the morphology of epoxy/SWCNT thin films was characterized by Raman and optical microscopy. The Raman spectrum of the SWCNTs has a strong Raman band at 1580–1590 cm^{-1}, called the G band,[36] which corresponds predominantly to stretching C—C vibrations with eigenvectors tangential to the nanotube surface. On the other hand, the epoxy matrix in the samples gives structureless Raman responses having mostly a fluorescence origin. This makes Raman microscopy an ideal tool for characterizing the dispersion of epoxy/SWCNT nanocomposites. Two types of Raman images produced from the hyperspectral cube are presented. One way to visualize the carbon nanotube dispersion is to plot the G-band Raman intensity distribution over the scanned area. In another approach, the reference Raman spectra of SWCNTs and the epoxy matrix are used to deconvolute the spectra contained in the hyperspectral cube to two components and present their distribution in a single Raman image. The first type of Raman imaging displays better regions with a high concentration of nanotubes in the sample, whereas the second one depicts improvements over those containing small amounts of SWCNTs.

The spatial resolution of the Raman images is determined by the size of the focused laser beam, which is diffraction limited. However, the Raman images recorded at sampling steps smaller than the laser spot size have a higher contrast than those obtained at the native resolution. A comprehensive description of the Raman imaging of SWCNTs can be found elsewhere.[37]

Figure 2(a) presents the optical image of a 80 × 80 μm^2 scanned area on the surface of an epoxy/P-

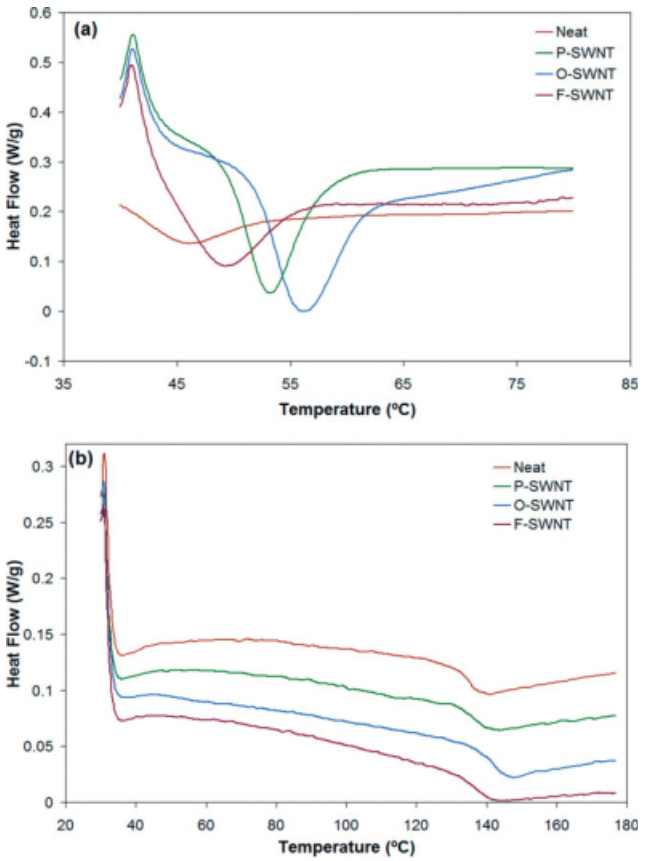

Figure 5 DSC thermograms of (a) about 50% and (b) 100% cured thin films. [Color figure can be viewed in the online issue, which is available at www.interscience.wiley.com.]

SWCNT (0.5 wt %) nanocomposite thin-film sample. The reference Raman spectra of the carbon nanotubes and epoxy matrix used for deconvolution of the hyperspectral cube are displayed in Figure 2(b). The Raman image showing the nanotubes (orange color) and epoxy (green color) distribution is given in Figure 2(c), and the G-mode intensity distribution is shown in Figure 2(d). Figures 3 and 4 display the Raman images of the epoxy/O-SWCNT (0.5 wt %) and epoxy/F-SWCNT (0.5 wt %) nanocomposites, respectively, collected under the same conditions as the ones shown in Figure 2.

The Raman images shown in Figures 2–3 demonstrate a gradual improvement of SWCNT dispersion going from P-SWCNTs to O-SWCNTs. The epoxy/P-SWCNT nanocomposite thin film exhibited the lowest degree of dispersion among the tested samples. The SWCNTs were aggregated at 10–50 μm in size, and substantial regions of the nanocomposite were free of SWCNTs. The SWCNT distribution within the agglomerates was highly inhomogeneous, and the SWCNTs were differently strained. Given the dependence of the G-band position on the nanotubes strain,[38,39] we estimated that the difference in strain between the outer carbon nanotubes in an agglomerate and those in the core was about 0.4%.

The oxidation of the SWCNTs apparently helped to improve their dispersion in the epoxy matrix, as shown in Figure 3. The distribution remained uneven, but the O-SWCNTs were dispersed practically in the entire volume of the nanocomposite thin film, leaving only small pockets of pure epoxy material.

The epoxy/F-SWCNT nanocomposite thin film exhibited the best dispersion among the three samples. The Raman images in Figure 4 demonstrate the remarkably smooth distribution of the F-SWCNT in the nanocomposite with some concentration irregularities, shown in Figure 4(d), below 1 μm in size. The results presented in Figure 4 show that the PAMAM G0 F-SWCNTs led to a high degree of SWCNT dispersion at a micrometer length scale and nanocomposites with far better quality than those produced with P-SWCNTs or O-SWCNTs. These findings were consistent with an earlier study on SWCNT dispersion due to surface functionalization using scanning electron microscopy and transmission electron microscopy.[35]

Properties of the thin films

Both the B-stage-cured thin-film samples and fully cured thin-film samples were characterized by DSC, as shown in Figure 5. The DSC thermograms in Figure 5(a) show that the B-stage-cured epoxy/SWCNT thin films had a melt range of about 50–57°C. Such a melt range ensured that the B-staged thin films remained stable at room temperature. Meanwhile, they could be easily processed upon heating. Such a property facilitated their subsequent VARTM processing.

TABLE II
Mechanical Properties of the Bulk Epoxy/SWCNT Nanocomposites (0.5 wt %)

Property	Neat epoxy	Epoxy/ P-SWCNT	Epoxy/ O-SWCNT	Epoxy/ F-SWCNT
Young's modulus (GPa)	2.77 ± 0.01	2.84 ± 0.05	3.17 ± 0.01	3.21 ± 0.15
Tensile strength (MPa)	60.1 ± 5.6	74.2 ± 0.5	76.5 ± 3.9	82.7 ± 3.2
Elongation (%)	1.98 ± 0.22	2.57 ± 0.18	2.97 ± 0.40	4.88 ± 0.91
K_{IC} (MPa $m^{1/2}$)	0.78 ± 0.01	0.76 ± 0.03	0.83 ± 0.05	0.93 ± 0.04

K_{IC}, Mode-I critical stress intensity factor.

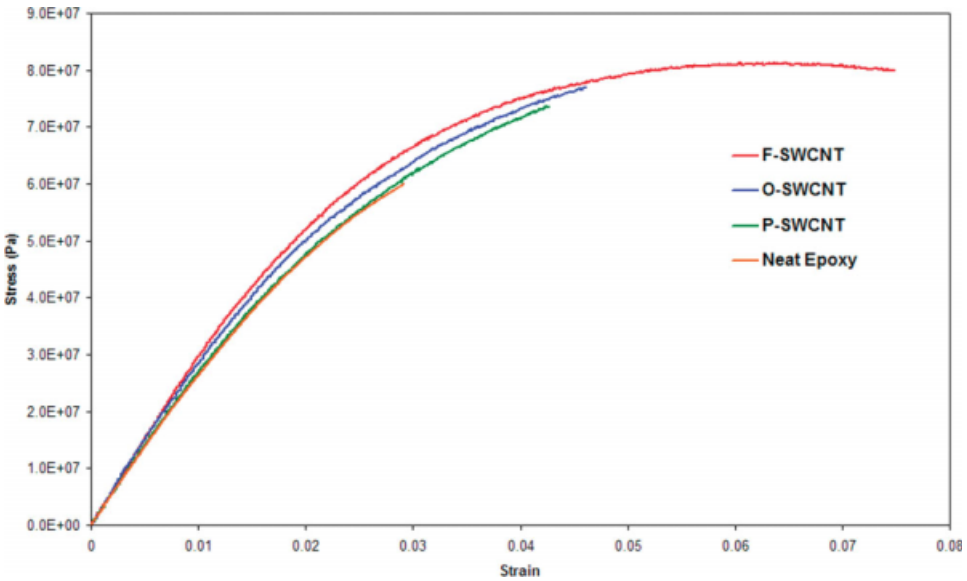

Figure 6 Tensile curves of the neat epoxy and epoxy/SWCNT nanocomposites. [Color figure can be viewed in the online issue, which is available at www.interscience.wiley.com.]

The DSC characterization of the fully cured thin films presented in Figure 5(b) showed that there was a minor variation in T_g from 136 to 144°C among the four film samples. Such a small variation was observed earlier and was believed to be due to (1) the trapping of the curing agent around the SWCNT bundles, (2) the side reactions of the curing agent with O-SWCNTs, or (3) the side reactions of the curing agent with the PAMAM dendrimers. All of these possibilities would have led to the alteration of the curing stoichiometric ratio and, thus, a minor variation in T_g.[35]

Tensile testing was performed to evaluate the effect of the SWCNT treatment on the mechanical properties of the epoxy nanocomposites. The key tensile properties are listed in Table II, and the tensile curves for all of the samples are shown in Figure 6. The results show that the incorporation of P-SWCNTs improved the Young's modulus and tensile strength of the epoxy by 3 and 23%, respectively. The limited improvement in the tensile properties was believed to be due to the poor SWCNT dispersion in the epoxy matrix, as shown in Figure 2. Oxidation of the SWCNTs led to a much better dispersion effect, and thus, the mechanical properties of the epoxy/O-SWCNTs were further improved. The incorporation of F-SWCNTs led to the best overall reinforcement effect in the modulus and strength by 16 and 35%, respectively. The tensile properties of the nanocomposite samples showed a good correlation with the level of dispersion of SWCNTs in the epoxy matrix. This study suggests that, as expected, a better dispersion of SWCNTs in the epoxy results in better improvements in the mechanical properties. The much higher elongation at break for the epoxy/F-SWCNT nanocomposite compared to the neat epoxy signified that the sizes of the SWCNT domains were smaller than the critical flaw size for the epoxy. Furthermore, the addition of PAMAM as a surface modifier for SWCNTs might have altered the epoxy curing and matrix properties. These data were the bulk properties of the nanocomposites. If the SWCNTs could be better aligned in the thin-film samples, the thin films would exhibit an even better improvement in mechanical properties along the SWCNT orientation.

The B-stage-cured thin films prepared in this study were successfully used as interleaves in composite laminates for VARTM processing. Well-integrated, good quality composites panels were prepared. The B-staged thin-film approach is an easy and practical way to introduce well-dispersed SWCNTs into locations of interest in composites. Their effect on the mechanical performance of carbon-fiber-reinforced composites, including interlaminar strength and delamination resistance, will be presented in the near future. Applications concerning microelectronic packaging and conductive coating of these thin films will soon be pursued.

CONCLUSIONS

B-staged epoxy/SWCNT nanocomposite thin films were successfully prepared. A high degree of dispersion of SWCNTs in the epoxy thin films was achieved. The Raman microscopy investigation indicated that the degree of dispersion dramatically increased as the SWCNTs were oxidized and functionalized by PAMAM G0 dendrimers. A high degree of dispersion of SWCNTs throughout the

preparation of the epoxy/SWCNT nanocomposite thin films yielded high-quality B-staged epoxy/SWCNT nanocomposite thin films. The degree of cure for the B-staged thin films was monitored and determined by DSC. The B-stage thin films with 50% cure gave satisfactory properties for VARTM processing to help enhance the mechanical properties of the laminated composites. This finding suggests that these epoxy/SWCNT nanocomposite thin films can be easily used as interleaves for VARTM composite laminate applications.

The authors thank Tony Golato of Hexcel for providing release paper for this study.

References

1. Iijima, S. Nature 1991, 354, 56.
2. Ebbesen, T. W. Annu Rev Mater Sci 1994, 24, 235.
3. Bernholc, J.; Brenner, D.; Buongiorno Nardelli, M.; Meunier, V.; Roland, C. Annu Rev Mater Res 2002, 32, 347.
4. Terrones, M. Annu Rev Mater Res 2003, 33, 419.
5. Dresselhaus, M. S.; Dresselhaus, G.; Jorio, A. Annu Rev Mater Res 2004, 34, 247.
6. Thostenson, E. T.; Ren, Z.; Chou, T.-W. Compos Sci Technol 2001, 61, 1899.
7. Yu, M.-F.; Files, B. S.; Arepalli, S.; Ruoff, R. S. Phys Rev Lett 2000, 84, 5552.
8. Nikolaev, P.; Bronikowski, M. J.; Bradley, R. K.; Rohmund, F.; Colbert, D. T.; Smith, K. A.; Smalley, R. E. Chem Phys Lett 1999, 313, 91.
9. Thess, A.; Lee, R.; Nikolaev, P.; Dai, H.; Petit, P.; Robert, J.; Xu, C.; Lee, Y. H.; Kim, S. G.; Rinzler, A. G.; Colbert, D. T.; Scuseria, G. E.; Tomanek, D.; Fischer, J. E.; Smalley, R. E. Science 1996, 273, 483.
10. Hone, J.; Llaguno, M. C.; Biercuk, M. J.; Johnson, A. T.; Batlogg, B.; Benes, Z.; Fischer, J. E. Appl Phys A 2002, 74, 339.
11. Xie, X.-L.; Mai, Y.-W.; Zhou, X.-P. Mater Sci Eng Rep 2005, 49, 89.
12. Moniruzzaman, M.; Winey, K. I. Macromolecules 2006, 39, 5194.
13. Liu, P. Eur Polym J 2005, 41, 2693.
14. Zhu, J.; Kim, J.; Peng, H.; Margrave, J. L.; Khabashesku, V. N.; Barrera, E. V. Nano Lett 2003, 3, 1107.
15. Zhu, J.; Peng, H.; Rodriguez-Macias, F.; Margrave, J. L.; Khabashesku, V. N.; Imam, A. M.; Lozano, K.; Barrera, E. V. Adv Funct Mater 2004, 14, 643.
16. Gong, X.; Liu, J.; Baskaran, S.; Voise, R. D.; Young, J. S. Chem Mater 2000, 12, 1049.
17. Bhattacharyya, A. R.; Sreekumar, T. V.; Liu, T.; Kumar, S.; Ericson, L. M.; Hauge, R. H.; Smalley, R. E. Polymer 2003, 44, 2373.
18. Shofner, M. L.; Khabashesku, V. N.; Barrera, E. V. Chem Mater 2006, 18, 906.
19. Du, F.; Scogna, R. C.; Zhou, W.; Brand, S.; Fischer, J. E.; Winey, K. I. Macromolecules 2004, 37, 9048.
20. Sreekumar, T. V.; Liu, T.; Min, B. G.; Guo, H.; Kumar, S.; Hauge, R. H.; Smalley, R. E. Adv Mater 2004, 16, 58.
21. Zhang, X.; Liu, T.; Sreekumar, T. V.; Kumar, S.; Moore, V. C.; Hauge, R. H.; Smalley, R. E. Nano Lett 2003, 3, 1285.
22. Sue, H. J.; Jones, R. E.; Garcia-Meitin, E. I. J Mater Sci 1993, 28, 6381.
23. Groleau, M. R.; Shi, Y. B.; Yee, A. F.; Bertram, J. L.; Sue, H. J.; Yang, P. C. Compos Sci Technol 1996, 56, 1223.
24. Lee, S.-H.; Noguchi, H.; Kim, Y.-B.; Cheong, S.-K. J Compos Mater 2002, 36, 2153.
25. Lee, S.-H.; Noguchi, H.; Kim, Y.-B.; Cheong, S.-K. J Compos Mater 2002, 36, 2169.
26. Derkowski, B. J.; Sue, H.-J. Polym Compos 2003, 24, 158.
27. Kishi, H.; Kuwata, M.; Matsuda, S.; Asami, T.; Murakami, A. Compos Sci Technol 2004, 64, 2517.
28. Fan, Z.; Alms, J.; Advani, S. G. In Proceedings of the 20th Annual Technical Conference American Society for Composites, Philadelphia, American Society for Composites: Dayton, Ohio, 2005; p 159.
29. Kim, J.; Barrera, E. V.; Armeniades, C. D. In International SAMPE Technical Conference; Society for the Advancement of Material and Process Engineering: Dayton, OH, 2003; Vol. 35, p 510.
30. Zhu, J.; Imam, A.; Crane, R.; Lozano, K.; Khabashesku, V. N.; Barrera, E. V. Compos Sci Technol 2007, 67, 1509.
31. Xu, X.; Thwe, M. M.; Shearwood, C.; Liao, K. Appl Phys Lett 2002, 81, 2833.
32. Xu, N. S.; Wu, Z. S.; Deng, S. Z.; Chen, J. J Vac Sci Technol B 2001, 19, 1370.
33. Cao, Q.; Xia, M.-G.; Shim, M.; Rogers, J. A. Adv Funct Mater 2006, 16, 2355.
34. Aglan, A.; Allie, A.; Ludwick, A.; Koons, L. Surf Coat Technol 2007, 202, 370.
35. Sun, L.; Warren, G. L.; O'Reilly, J. Y.; Everett, W. N.; Lee, S. M.; Davis, D.; Lagoudas, D.; Sue, H. J. Carbon 2008, 46, 320.
36. Dresselhaus, M. S.; Eklund, P. C. Adv Phys 2000, 49, 705.
37. Hadjiev, V. G.; Arepalli, S.; Nikolaev, P.; Jandl, S.; Yowell, L. Nanotechnology 2004, 15, 562.
38. Hadjiev, V. G.; Iliev, M. N.; Arepalli, S.; Nikolaev, P.; Files, B. S. Appl Phys Lett 2001, 78, 3193.
39. Hadjiev, V. G.; Lagoudas, D. C.; Oh, E. S.; Thakre, P.; Davis, D.; Files, B. S.; Yowell, L.; Arepalli, S.; Bahr, J. L.; Tour, J. M. Compos Sci Technol 2005, 66, 128.